

# Analysis of Air Flow Around the Painting Line for Dust Reduction: An Experimental and Numerical Study


 Open  
Access

 Muhammad Hafizan Yosri<sup>1</sup>, Pauziah Muhamad<sup>1,\*</sup>, Lee Kee Quen<sup>1</sup>, Norfazrina Mohd Yatim<sup>2</sup>
<sup>1</sup> Intelligent Dynamics & System Research Lab, Malaysia-Japan International Institute of Technology, Universiti Teknologi Malaysia, 54100 Kuala Lumpur, Malaysia

<sup>2</sup> Department of Mechanical Engineering, Kulliyah of Engineering, International Islamic University Malaysia, 50728 Kuala Lumpur, Malaysia

## ARTICLE INFO

### Article history:

Received 22 July 2020

Received in revised form 20 September 2020

Accepted 23 September 2020

Available online 29 September 2020

## ABSTRACT

The repair of paint work defects in the painting production process is done by running the parts through the painting process again. It is done together with the requisite quality control routines and involves a very large proportion of the operating costs. The dust defect which ranges between 40% to 50% is found to be the top and highest rejection at the painting line. Hence, this paper is focused to identify the effectiveness of applying Computational Fluid Dynamic (CFD) to identify the air flow and the turbulence pattern to investigate the movement and the dust particle concentration in painting line. Renormalization Group (RNG)  $k-\epsilon$  turbulence model is used in CFD to predict the particles' movement and concentration. Five new models including the current painting line design are proposed and tested. The painting line model labelled as Model F is found to be the best model to minimize and reduce the dust particle concentration inside the painting line environment with 96.01% of percentage particle is flushed out at air velocity of 0.1 m/s. Along with results from numerical simulation using CFD, the experimental data is also collected using an air flow meter in a small-scale model painting line. Both data from experiment and CFD simulation are analysed and compared in order to measure the effectiveness of the result. The average relative error for Model F is recorded at 4.76%. The results from this study is recommended to be considered as one of the benchmarks for future design of automotive painting line.

### Keywords:

Computational Fluid Dynamic (CFD); RNG

 $k-\epsilon$  model; Particle concentration;

Automotive Painting Line

Copyright © 2020 PENERBIT AKADEMIA BARU - All rights reserved

## 1. Introduction

Recently, the top and highest rejection for almost all painting lines in automotive industry is contributed from dust that ranges from 40% to 50%. Thus, it has become a critical issue to the coating industries as dust and fibre has great effects on the appearance issue. The repair of paint work defects where the parts are run through the process again, together with the requisite quality control routines, accounts for a very large portion of the operating costs. Contamination contributed by dust

\* Corresponding author.

E-mail address: [pauziah.kl@utm.my](mailto:pauziah.kl@utm.my) (Pauziah Muhamad)

<https://doi.org/10.37934/cfdl.12.9.3650>

particles has been identified as the highest rejection in automotive painting line and it has become crucial to understand the dust particles movement and its concentration in the painting line environment. Figure 1 describes the rejection breakdown occurred in one company's painting line. Prior to this, Combat Coating (M) Sdn Bhd [1] suggested an ionizer device to be installed before the primer coating process as to neutralize the substrate in order to reduce the dust particle attraction to the painted surface. However, the results show only a small reduction of 0.4% rejection contributed by foreign particles [2]. Thus, in order to reduce the airborne contamination that is contributed by dust particles, Computational Fluid Dynamic (CFD) is further utilized to understand the turbulence and the air flow pattern that will affect the dust particles concentration in the painting line environment.

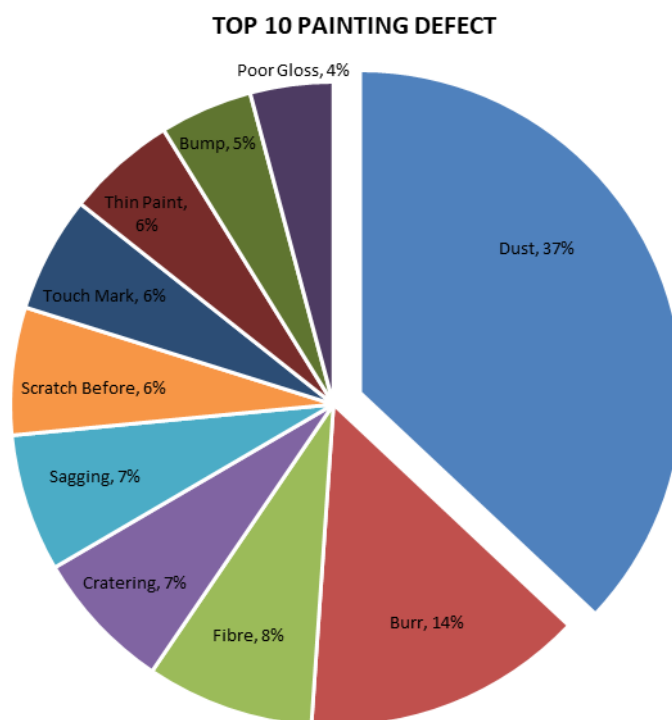


**Fig. 1.** Pie chart of defect distribution for painting line defect in 2019 [2]

### 1.1 Defect Phenomenon in Actual Painting Parts

Initial investigation by Combat Coating (M) Sdn Bhd [2], found that the contamination comes from two main sources as mentioned in Figure 2.

- a. Material: improper cleaning process at the painting substrate before entering the painting process. The dirt or stain from the handling processes had contaminated the painting substrate even after the wiping process is done.
- b. Environment effect: foreign particles in the painting line environment is circulated then follows the air flow pattern. Thus, the concentration of the foreign particles has contaminated the painting parts due to the turbulence occurrence around the painted surface.



Fig. 2. Source of contamination of dust and in painting line [1]

### 1.2 Computational Fluid Dynamic (CFD)

CFD application is widely used to simulate the air flow field in indoor environment such as in the clean room of the Liquid Crystal Display (LCD) industry and classroom. CFD helps to provide a good result which can improve the air flow quality as suggested by Adisorn and Jatuporn [3]. An example of CFD application is from Jatuporn [4], the author had successfully predicted and characterised the air flow pattern inside a Hard Disk Drive (HDD) of a production microenvironment line using CFD. This finding propelled the same basis principle to be applied due to its similarity of the ventilation system between the clean room and the automotive painting line. Both have the same principle which applied the air inlet and outlet systems to create a laminar air flow system in order to flush the contamination out from the environment as describe by Tongsri and Pongkom [5]. In other article of Jatuporn *et al.*, [6], the authors are able to find the suitable location to place the air circulating occurrence after running CFD simulation and has examined the air flow pattern, dust particles trajectories and its movement inside the HDD assembly line. In addition, the successful work from Kamsah *et al.*, [7] has shown an excellent result from CFD implementation to measure the dust particles concentration in a hospital operating room. From these studies, the design of a suitable ventilation equipment, the positioning of air supply and extraction ducts plus the optimal location of working areas and machine can benefit from the use of the CFD as suggested by Seo *et al.*, [8].

### 1.3 Dust Particles Movement in Indoor Environment

Air distribution in an enclosed environment can be driven by different forces such as natural wind, mechanical fan or thermal buoyancy. The combination of these flow mechanisms creates complex indoor air flow characteristics with impingement, separation, circulation, reattachment and buoyancy as illustrated in Figure 3. The corresponding flow regimes may span from laminar to transitional, and to turbulent flows or a combination of all flow regimes under transient conditions. The complexity of indoor air flow makes experimental investigation extremely difficult and expensive especially if conducted in actual manufacturing processes. Air flow system is designed to minimize the risk of dust particles falling below the critical velocity and attached on the surface. Hence, the design of the air flow system should consider the equipment and other fixtures position. Xia *et al.*, [9] found that the random position of the operator and mobile equipment can adversely affect the system performance.

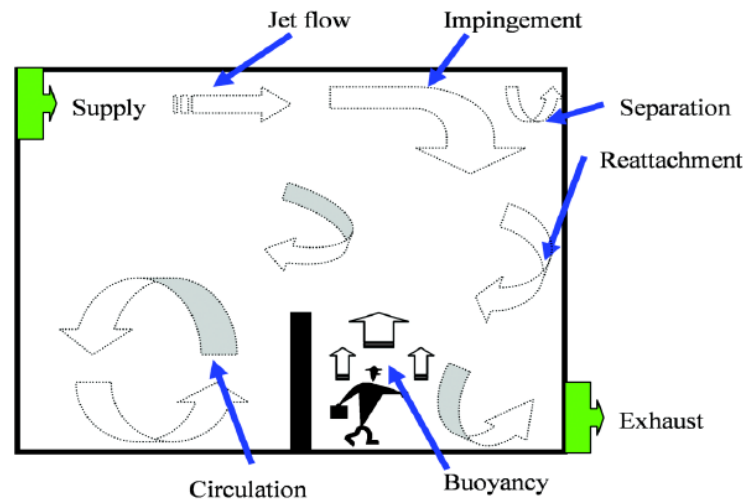


**Fig. 3.** Typical flow characteristics in an enclosed environment with various flow mechanisms

Jatuporn *et al.*, [4] revealed that the optimum air speed where the speed resulting in the lowest dust particle counts is in the range of 0.35 m/s to 0.55 m/s in consideration of surrounding activities of the operators. Based on this study, two assumptions have been made where the clean air from the Fan Filter Unit (FFU) should be able to block the airborne from outside and purge out the dust particles that is generated from inside. The result implied that higher air speed will flush out more dust particles from the painting line environment.

#### 1.4 Turbulence Model: RNG $k$ - $\epsilon$ Model

The standard  $k$ - $\epsilon$  model potentially fails to predict accurately the air flow in non-isotropic turbulence even though it has been widely applied and provides a modest calculation speed as mentioned by Norton *et al.*, [10]. Christian *et al.*, [11] found that, in order to improve this drawback, two upgraded models namely the RNG  $k$ - $\epsilon$  and the Realizable  $k$ - $\epsilon$  models are developed. The RNG  $k$ - $\epsilon$  turbulence model is developed to improve the  $k$ - $\epsilon$  model's deficiency in determining the turbulence kinetic energy. This improved model has been added an extra source term to the turbulence kinetic energy dissipation ( $\epsilon$ ) transport equation with different constants as compared to the standard  $k$ - $\epsilon$  model as describe by Caiqing *et al.*, [12]. The model is suggested by Yakhot *et al.*, [13] which generate better results as compared to the standard model that is commonly used in air flow simulation for indoor environments as mentioned by Sadrizadeh *et al.*, [14].

##### 1.4.1 Transport equations for the RNG $k$ - $\epsilon$ model

The RNG  $k$ - $\epsilon$  model for transport equations has a similar form to the standard  $k$ - $\epsilon$  model as defined in Eq. (1) and Eq. (2):

$$\frac{\partial}{\partial t}(\rho k) + \frac{\partial}{\partial x_i}(\rho k u_i) = \frac{\partial}{\partial x_j} \left[ \alpha_k \mu_{eff} \frac{\partial k}{\partial x_j} \right] + G_k + G_b - \rho \epsilon - Y_M + S_k \quad (1)$$

$$\frac{\partial}{\partial t}(\rho \epsilon) + \frac{\partial}{\partial x_i}(\rho \epsilon u_i) = \frac{\partial}{\partial x_j} \left[ \alpha_\epsilon \mu_{eff} \frac{\partial \epsilon}{\partial x_j} \right] + C_{1\epsilon} \frac{\epsilon}{k} (G_k + C_{3\epsilon} G_b) - C_{2\epsilon} \rho \frac{\epsilon^2}{k} - R_\epsilon + S_\epsilon \quad (2)$$

From above equations,  $G_k$  represents the generation of turbulence kinetic energy caused by the mean velocity gradients while  $G_b$  is the generation of turbulence kinetic energy caused by buoyancy.  $Y_M$  indicates the representation of the fluctuating dilatation in compressible turbulence to the overall dissipation rate. The quantities  $\alpha_k$  and  $\alpha_\epsilon$  are the inverse effective Prandtl numbers for  $k$  and  $\epsilon$ , respectively, while  $S_k$  and  $S_\epsilon$  are user-defined source terms.

**2. Methodology**

**2.1 Computational Fluid Dynamic (CFD)**

**2.1.1 Mechanical design proposal**

Six mechanical designs of ventilation system in automotive painting line including the existing design are tested in order to find the most effective ventilation system that is able to remove and flush out dust particles from the painting line environment. The ventilation system design is focused on the location, size and orientation of the fan exhaust (outlet system) in the painting line system. There are three factors being monitored in order to achieve the objective of the numerical simulation; air flow velocity, air flow vector and the dust particles concentration. In addition, four variables of air flow velocities are tested to find the most suitable velocity that matches with the design proposal in order to achieve dust particles reduction. Nonetheless, one main limitation factor is the machine capability where the air supply unit for the painting line can only supply air flow velocity with a range of 0.10 m/s to 0.50 m/s. The process flow for the simulation and experimental testing can be referred in Figure 4.

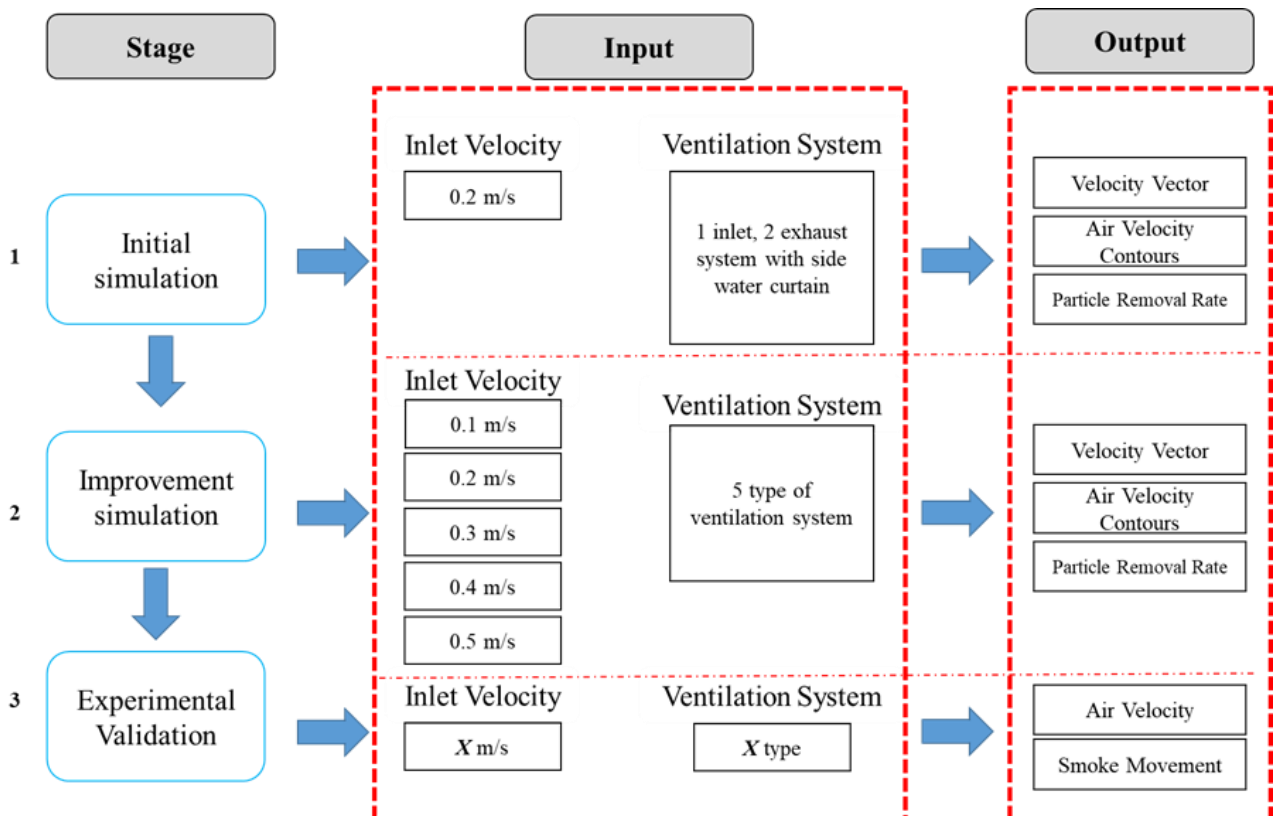
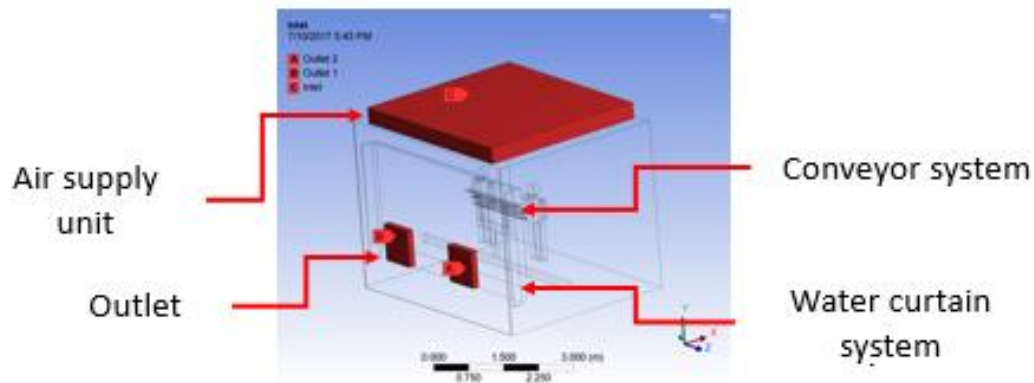


Fig. 4. Flow of simulation and experimental testing

### 2.1.2 Basic operation system of painting line

The automotive painting line has four basic components which enable the system to run effectively. The four components are the air supply unit (ASU), conveyor system, exhaust (outlet) and water curtain as shown in Figure 5. Detailed description of each component can be referred to Table 1. Figure 6 describes the design concept of six mechanical designs and the justification of the ventilation system in the painting line. The indication starts with alphabet A to F design proposals.

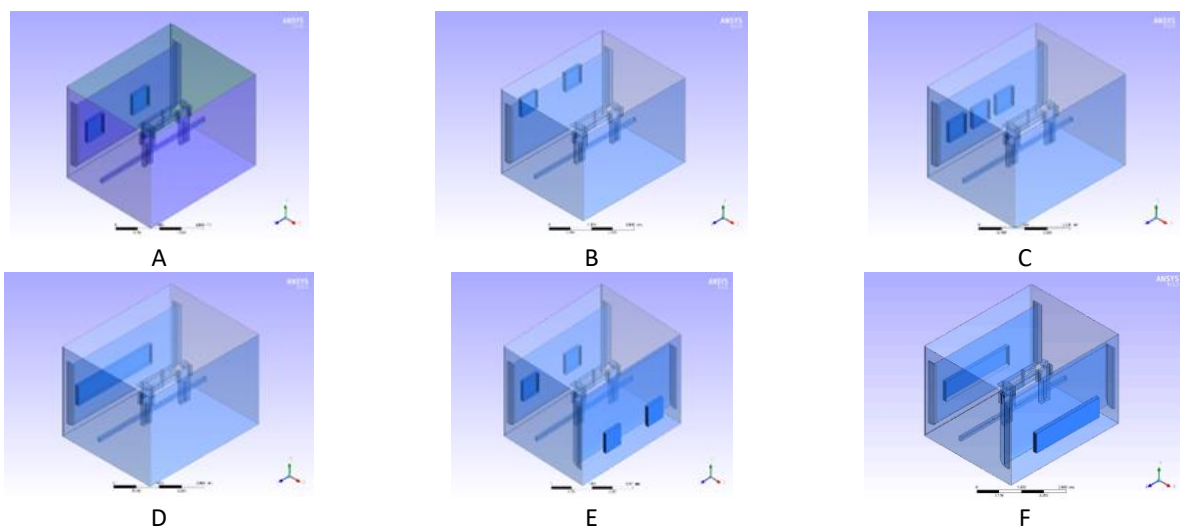


**Fig. 5.** Basic operation system of painting line

**Table 1**

Painting line main components description

Item	Description
Exhaust Fan (Outlet)	The outlet system where the air is circulation is taken out form the painting line
Conveyor system	The handling system to hold the part during painting process which consists of chain conveyor and painting jigs
Water curtain	Part of mechanical structure for exhaust system that function to collect the over spray residue inside the painting line environment
Air Supply Unit	The mechanism function to supply the air into the painting line that include fan unit, speed controller and power supply



A: Initial painting line design with two exhausts and water curtain system, B: Exhaust positioning at the top area of the water curtain, C: Additional exhaust positioning at the same area as initial design, D: Horizontal type of exhaust positioning at the same area as initial design, E: Similar to initial design with double exhaust and water curtain system, F: Two horizontal type of exhaust positioning at both sides of the painting line

**Fig. 6.** Mechanical design proposals for air ventilation system in automotive painting line

### 2.1.3 Parameter at boundary condition

The inlet conditions are set at multiple air velocity settings and the inlet turbulence intensity is 4%. The outlet condition is set as a constant pressure of zero. These conditions are consistent with Nielsen's test case [15]. The commercial software FLUENT 15.0.7 is used to perform the numerical simulations and a SIMPLE algorithm is selected to run the simulation. A second-order upwind scheme is used for discretizing the convection terms. Convergence criteria for the continuity and energy equations are set as 0.03. The particle movement in the ventilated system of painting line is simulated using anthracite particle by applying Lagrangian-based discrete random walk (DRW) model and the particle count is set at  $1 \times 10^6$ . The mesh structure with an average of 1700000 nodes from 6 different designs is chosen.

## 2.2 Experimental Set-up and Procedure

### 2.2.1 Painting line model configuration

The small-scale model of painting line has been developed from scale of 1:25 with the dimensions of 5.10 x 4.26 x 3.65 m (length x width x high) as described in Figure 7. The model consists of air supply unit (inlet), exhaust system (outlet), mannequin, painted part and conveyor system.

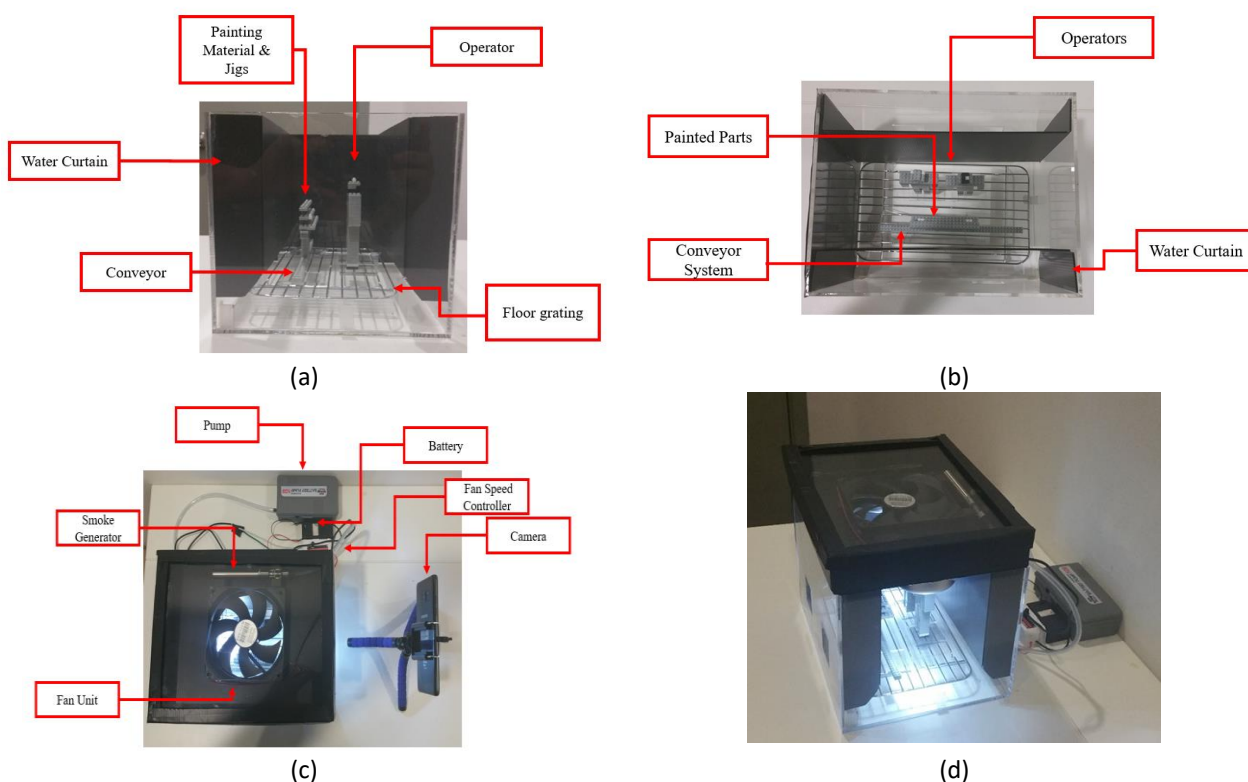


**Fig. 7.** Configurations of small-scale painting line model from (a) Side view, (b) Top view: Interior layout, (c) Top view: With ventilation system, and (d) Isometric view

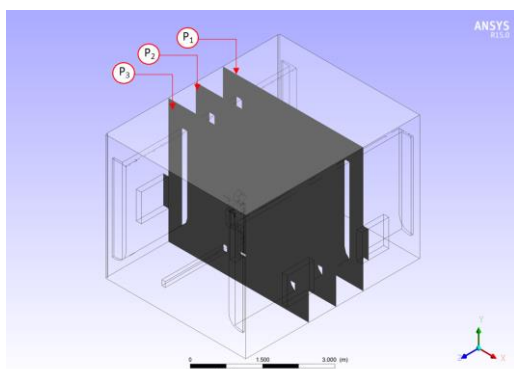
### 2.2.2 Measurement equipment

The hot-wire anemometer model Testo 405i is used to measure the air flow velocities inside the small-scale painting line. This equipment has a measuring range from 0 to 30 m/s with an accuracy of  $\pm 0.1$  m/s. The measured data is analysed and summarized via Testo Smart Probes application. This

equipment has an extendable 400 mm telescopic shaft which enables the user to collect data at small and narrow area.

### 2.2.3 Measurement procedure

Data collection for experimental testing is divided into two types of data which include the variable data and attribute data. For variable data, the air flow velocity is measured from the small-scale model for both current (initial) and improved models. The measuring points are fixed at three parallel vertical planes with different distance that covers the working area where the painted parts and the sprayer are located. The measuring planes P1, P2 and P3 as described in Figure 8 are located at 2.0 m, 2.4 m and 2.8 m from Z axis respectively. These are the critical area where the painting process is done inside the painting line. As for the attribute data, the smoke visualization which represents the air flow pattern is monitored. The visual movement of the smoke will be compared with numerical data attained from CFD simulation as done by Nielsen *et al.*, [16]. Finally, the cycle time for each measured point is taken at 120 seconds to get the average and consistent value referring to the practice by Zhixiang *et al.*, [17].



Plane	Location from Z-Axis (m)
P1	2.0
P2	2.4
P3	2.8

Fig. 8. Location of measuring points for data collection

## 3. Results and Discussion

### 3.1 Numerical Simulation Result for Painting Line Model Using CFD

From the CFD simulation results shown in Figure 9, Model F provides the most efficient dust particles removal rate followed by Models E, C, D, A and B. At air flow speed of 0.1 m/s, Model F provides 96.01% of dust particles removal rate compared to the existing initial Model A with 80.45% of dust particles removal rate at an initial air flow input of 0.2 m/s.

The dust particles concentration will increase significantly with the turbulence occurrence in the painting line environment. Meanwhile, it is observed that there is no correlation on the reduction of the dust particles in the painting line environment when the input air flow speed increases. In summary, the efficiency of the dust particles removal rate is highest at input of 0.1 m/s air flow speed, except for Models A and E. It is seen from the simulation that the higher the input of air flow getting into the painting line, the more turbulence occurrence is generated which contributes to high dust particles concentration inside the painting line environment.

Essentially, the simulation models can be categorized into two main categories; single-sided and double-sided ventilation systems. Models E and F fall under the double-sided ventilation system while the rest (Models A, B, C and D) are single-sided ventilation systems. It is seen from the dust particles removal rate that the double-sided ventilation system gives better result over the single-sided ventilation system with an increase of 11.86% of removal rate.

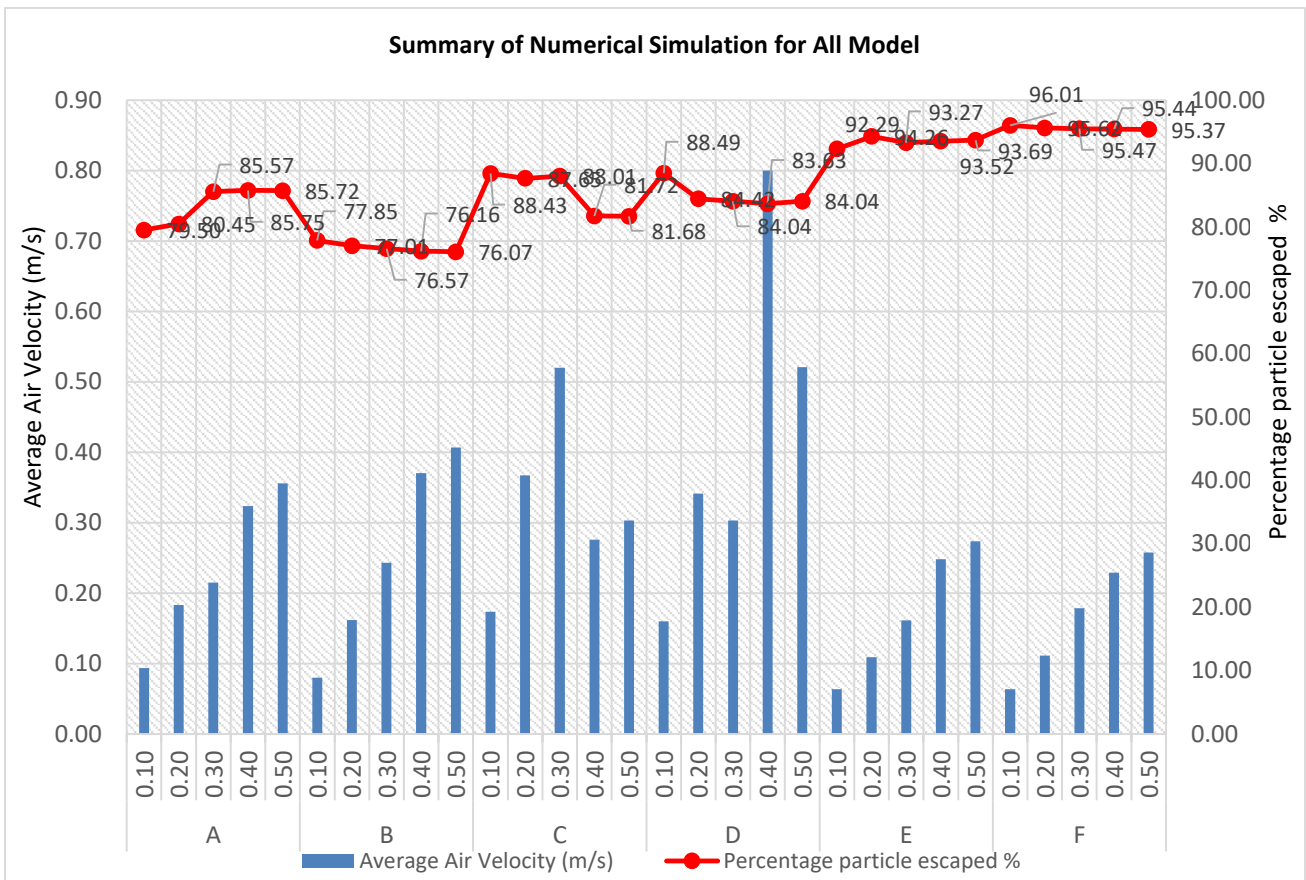


**Fig. 9.** Summary of average air velocity (histogram) and percentage of particle escaped (line chart) from numerical simulation for each painting line model

It is understood from the simulated result that the single-sided ventilation system generates higher turbulence occurrence compared to that of the two-sided ventilation system. The two-sided ventilation system produces a more stable and laminar air flow which provides better removal efficiency rate. As for Models E and F, the positioning of two ventilation systems at both sides of the painting line generates laminar air flow which helps stabilizes the air flow movement. The design of Model F is an improved version of Model E where the outlet of the system is enlarged to increase the dust particles removal rate. With a two-sided outlet, Model F is able to stabilize the air flow movement with symmetrical air flow vector while for Model A shows the air flow moves across the painting line and go through the painted part.

Comparatively, the single-sided ventilation system will generate turbulence that carries together the dust particles within the air and circulates around the painted surface. It is seen that there is no significant improvement in terms of turbulence occurrence and dust particles removal rate for the new single-sided ventilation system when compared to the initial Model A. The change of location, additional outlet location and parameter setting of air speed has no effect in improving the ventilation system. Moreover, the condition becomes worst especially for Model B where the outlet position is located at the upper level of the painting line causing the air flow to split at the centre area where the painted part is located. This situation creates turbulence and the dust particles will circulate at the centre area. Thus, the Model B provides less efficient dust particles removal rate compared to other ventilation systems.

Based on the particle tracking results from the CFD simulation, Model F provides the most prevalence result in terms of the percentage of dust particles escaped at 96.01% with the average air flow velocity at 0.06 m/s from the 0.1 m/s air flow input. However, the efficiency of the ventilation system in reducing the dust particles begins to deteriorate when the input air velocity increases from 0.2 m/s to 0.5 m/s. In opposite of that, only Model A provides positive result when the input air velocity is increased gradually to the maximum value of 0.5 m/s.

### 3.1.1 Numerical simulation result: Model A (Current mechanical design at air flow velocity 0.2 m/s)

The simulated air flow in Figure 10 shows the intensity and concentration of dust particles at the critical area for Model A due to the turbulence occurrence around the painted part. The movement of air flow which carries together the injected particles will increase the dust particles concentration within the turbulence occurrence area. Based on the observation of the overall air flow movement inside the painting line environment, the turbulence and dust particles concentration in front of the sprayer and the painted parts are among the worst conditions compared to other locations. With an average of 0.18 m/s air velocity input, the movement of the air vector is flowing across the painted material before flushes out through the water curtain and gets expelled by the exhaust outlet.

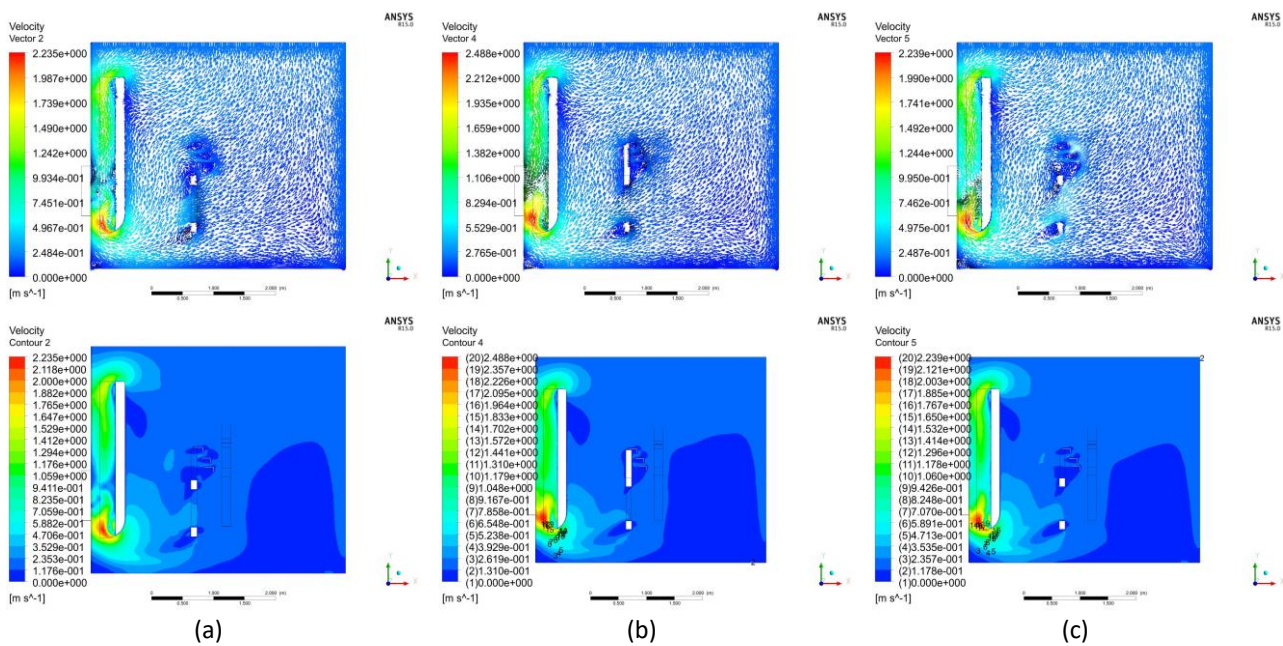


**Fig. 10.** Initial painting line design with two exhaust and water curtain for Model A. Air velocity vector (upper side) and velocity contour (lower side) using air velocity input of 0.2 m/s at plane position (a) 2.0 m, (b) 2.4 m and (c) 2.8 m

### 3.1.2 Numerical simulation result: Model F (Improved design at air flow velocity 0.1 m/s)

From the simulated result in Figure 11 for Model F, the air flow velocity at 0.1 m/s generates the most effective particle escaped of 96.01% compared to other parameters. The higher percentage indicates better efficiency of ventilation system to remove the dust particles from the environment. From the simulated result, it is found that there is no significant improvement in terms of particle escaped when the air flow velocity is increased from 0.1 m/s to 0.5 m/s. The air flow vector indicates that the turbulence occurrence is starting to intensify around the painted surface area concurrently with increasing air flow velocity. The average value for air velocity input of 0.10 m/s is recorded at

0.06 m/s. It is seen that the air flow vector for Model F is similar to laminar flow which has less turbulence occurrence around the painted part surface. The double-sided ventilation system helps to generate better air flow pattern that stabilizes the air flow movement by avoiding the turbulence occurrence. Hence, the risk of the dust particles to circulate and fall down towards the painted surface is very less compared to other models.

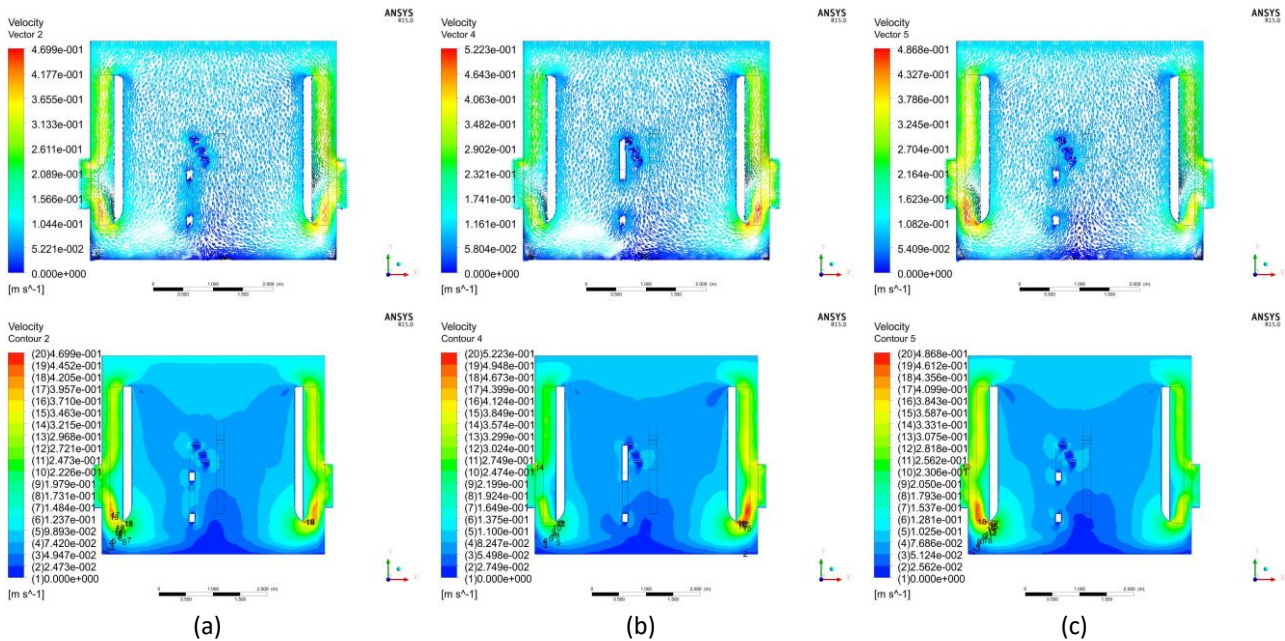


**Fig. 11.** Double horizontal exhaust and water curtain system for Model F. Air velocity vector (upper side) and velocity contour (lower side) using air velocity input of 0.1 m/s at plane position (a) 2.0 m, (b) 2.4 m and (c) 2.8 m

### 3.2 Small-Scale Experiment

#### 3.2.1 Air velocity verification

The average value of air velocity input obtained from the three test points in the painting line Models A and F is compared in order to verify the simulation data against the actual experimental data. Model F with 0.1 m/s air velocity input is selected as the proposed new design of painting line since it provides the most efficient dust particles removal rate (96.01%) from the CFD simulation. Therefore, this model is selected as the benchmark for comparison with the experimental results of both Models A and F.

The experimental results of air velocity and the relative error with the simulation data for three critical planes in Models A and F are illustrated in Figure 12. For Model F at air velocity input of 0.1 m/s, the average relative error across the plane is recorded at 4.76%, while for Model A shows a much higher value at 7.22% at air velocity input of 0.2 m/s. From the experimental data, it shows that the parameter with the highest dust particles removal rate generates the lowest discrepancy in air flow velocity compared to the other parameters as observed in Model F. The accuracy between simulation and experimental value for both models decreases when the air velocity input is increased from 0.2 m/s to 0.5 m/s.

The main reason for the fluctuation is due to the variation of air velocity fluctuation specifically around the sprayer and the painted part. As seen from the simulated data, the turbulence occurrence is not evenly distributed throughout the cross-sectional plane which affect the fluctuation of the air velocity itself. Higher air flow velocity will escalate the turbulence occurrence thus increases the data

discrepancy during experimental testing. The data discrepancy might also be contributed by the turbulence occurrence around the air flow meter during the testing. As mentioned by Zhang [18], the experimental results within this range shows a good agreement with the simulation data and can be accepted for validation.

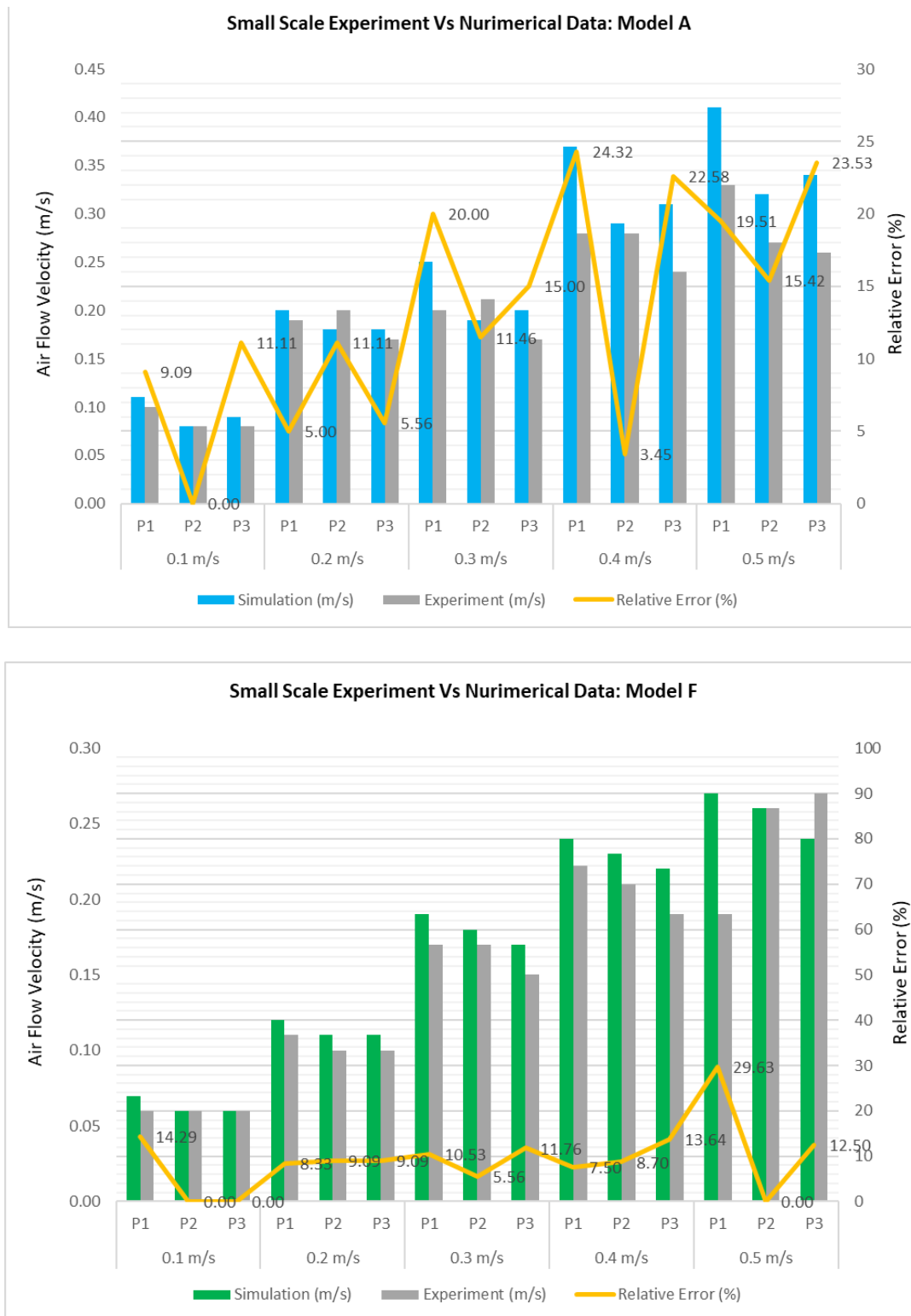


**Fig. 12.** Air velocity and its relative error between small-scale experiment against numerical data: Model A (top) and Model F (bottom)

### 3.2.2 Smoke visualization for air flow vector

Smoke visualization experimental testing (see, Figure 13) is conducted to visualize and verify the air flow vector generated inside the small-scale painting line. The air flow vector between numerical and experiment data is compared visually for both Models A and F. Based on visual observation of Model A, the air flow moves across the painting line environment from the input (ceiling filter) and goes down to the water curtain before getting removed out through the output (exhaust). A minor turbulence occurrence can be seen around the painted part, specifically in front of the sprayer. Based on visual monitoring, there is no visible change in terms of the air flow vector during smoke visualization monitoring at air velocity input of 0.2 m/s. As for Model F, the air flow vector is moving downwards from the input (ceiling filter) into the painting line environment and moves vertically down to the water curtain before being expelled out through the output (exhaust). This air flow condition shows good agreement with the numerical simulation data obtained from CFD. The air movement is similar to laminar flow which will create less turbulence occurrence around the painted part surface. There is no significant change in the air flow vector during the visual monitoring at air flow speed of 0.1 m/s.

From this observation, the double-sided ventilation system in the painting line can generate better air flow pattern by stabilizing the air flow vector thus evade the turbulence occurrence. In regard to that, the risk of the dust particles to circulate and fall down into the painted surface is minimal compared to the single-sided ventilation system. Despite that, Model A with a single-sided ventilation system shows minor turbulence occurrence around the painted parts. In actual environment, this turbulence may carry along dust particles within the air that circulates around the painted surface inside the painting line which can lead to contamination.

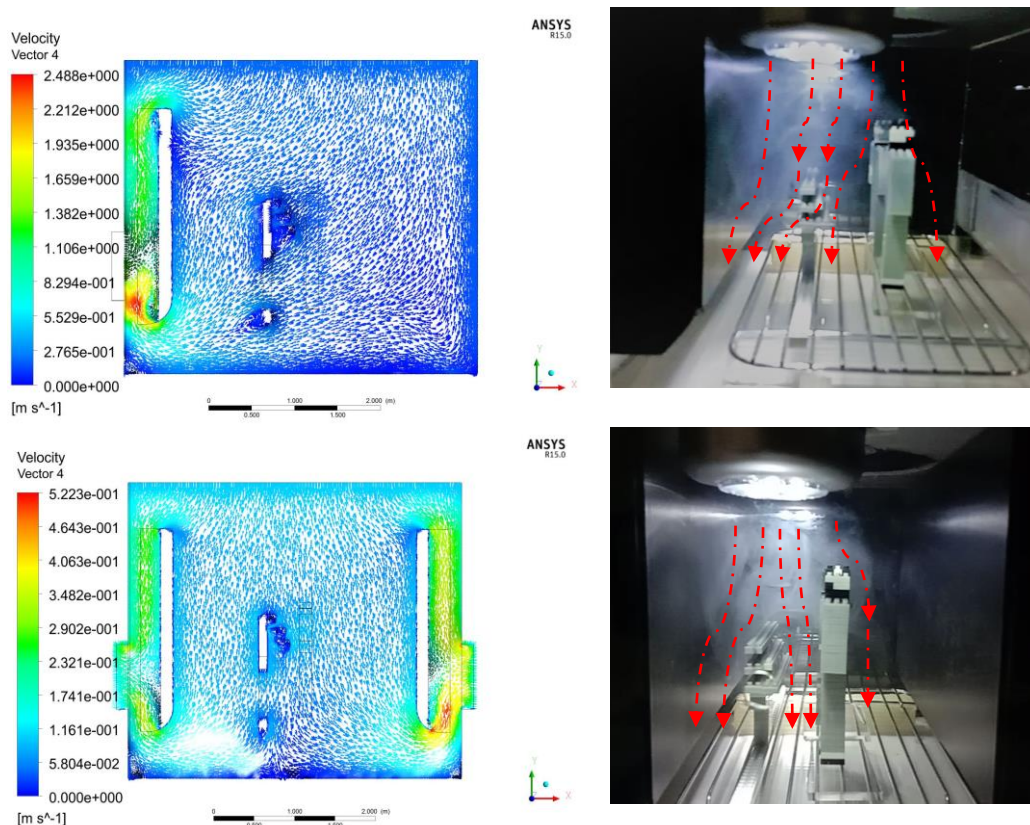


**Fig. 13.** Smoke visualization for air flow vector at air velocity of 0.2 m/s (initial condition) for Model A (top) and air velocity of 0.1 m/s for Model F (bottom)

#### 4. Conclusions

Five variables of air velocity have been used as input for air inlet to validate the performance of six painting line designs in order to flush and removed the dust particles that contributes to the painted part rejection. Referring to the CFD simulation results, Model F is the most efficient model in term of dust particles removal rate followed by Models E, C, D, A and B. Model F provides 96.01% of dust particles removal rate at 0.1 m/s air flow input while the initial Model A only has 80.45% of dust particles removal rate at 0.2 m/s of air flow input (current parameter). The dust particles concentration is increased significantly with the turbulence occurrence as referred to the dust particle removal rate. It is found that the increase of air flow speed shows no correlation on the reduction of the dust particles around the painted area. In most of the cases (except for Models A and E), the efficiency of dust particles removal rate is at highest value when the air flow parameter input is 0.1 m/s and started to deteriorate when the air flow is increased from 0.2 m/s to 0.5 m/s. Therefore, higher air flow input will generate more turbulence that contributes to high dust particles concentration in the painting line environment.

Small scale experiment has been conducted to verify and compared the actual air velocity with the numerical simulation data from CFD. In overall, air flow of 0.2 m/s has been selected as the benchmarking parameter value for model A while 0.1 m/s was choose for Model F. As for Model F at air velocity input of 0.1 m/s, the simulated value is in good agreement with the experimental value with an average discrepancy of 4.76%. Meanwhile, for Model A at air velocity input of 0.2 m/s, the average discrepancy is much higher at 7.22%. Hence, the relative error between numerical and experimental value in this study is considered good and acceptable for evaluation.

#### Acknowledgement

The authors are grateful to the Universiti Teknologi Malaysia (UTM) for providing the facility and technical advice during this research. Also, to the Ministry of Higher Education (MOHE) Malaysia under the FRGS Grant. The grant was managed by the Research Management Centre, Universiti Teknologi Malaysia: FRGS Fund No. FRGS/1/2018/TK03/UTM/02/10.

#### References

- [1] Combat Coating (M) Sdn Bhd. "Outgoing Quality Inspection Passrate Report." 2019.
- [2] Yosri, Muhammad Hafizan, Pauziah Muhamad, and Norfazrina Hayati Mohd Yatim. "Evaluation of Air Flow Pattern for Conceptual Design of Automotive Painting Line Using Computational Fluid Dynamic (CFD) for Better Dust Particle Reduction." *CFD Letters* 11, no. 2 (2019): 42-49.
- [3] Khaokom, Adisorn, and Jatuporn Thongsri. "Feasibility study for installing machine in production line to avoid particle contamination based on CFD simulation." In *IOP Conference Series: Materials Science and Engineering*, vol. 241. 2017.  
<https://doi.org/10.1088/1757-899X/241/1/012011>
- [4] Thongsri, Jatuporn, and Monsak Pimsarn. "Optimum airflow to reduce particle contamination inside welding automation machine of hard disk drive production line." *International journal of precision engineering and manufacturing* 16, no. 3 (2015): 509-515.  
<https://doi.org/10.1007/s12541-015-0069-2>.
- [5] Thongsri, Jatuporn, and Vana Pongkom. "A simulation of the number of particles trapped by the circulating filter of a hard disk drive and their trajectories." In *Applied Mechanics and Materials*, vol. 548, pp. 953-957. Trans Tech Publications Ltd, 2014.  
<https://doi.org/10.4028/www.scientific.net/AMM.548-549.953>.
- [6] Thongsri, Jatuporn. "A problem of particulate contamination in an automated assembly machine successfully solved by CFD and simple experiments." *Mathematical Problems in Engineering* 2017 (2017).  
<https://doi.org/10.1155/2017/6859852>.

- [7] Kamsah, Nazri, Haslinda Mohamed Kamar, Muhammad Idrus Alhamid, and Wong Keng Yinn. "Impacts of temperature on airborne particles in a hospital operating room." *Journal of Advanced Research in Fluid Mechanics and Thermal Sciences* 44, no. 1 (2018): 12-23.  
[http://www.akademiabaru.com/arfmtsv44\\_n1\\_p12\\_23.html](http://www.akademiabaru.com/arfmtsv44_n1_p12_23.html).
- [8] Seo, Il-hwan, In-bok Lee, Oun-kyeong Moon, Se-woon Hong, Hyun-seob Hwang, Jessie P. Bitog, Kyeong-seok Kwon, Zhangying Ye, and Jong-won Lee. "Modelling of internal environmental conditions in a full-scale commercial pig house containing animals." *Biosystems engineering* 111, no. 1 (2012): 91-106.  
<https://doi.org/10.1016/j.biosystemseng.2011.10.012>
- [9] Xia, Bin, and Da-Wen Sun. "Applications of computational fluid dynamics (CFD) in the food industry: a review." *Computers and electronics in agriculture* 34, no. 1-3 (2002): 5-24..  
<https://doi.org/10.1016/S0168-1699%2801%2900177-6>
- [10] Norton, Tomás, Da-Wen Sun, Jim Grant, Richard Fallon, and Vincent Dodd. "Applications of computational fluid dynamics (CFD) in the modelling and design of ventilation systems in the agricultural industry: A review." *Bioresource technology* 98, no. 12 (2007): 2386-2414.  
<https://doi.org/10.1016/j.biortech.2006.11.025>
- [11] Heschl, Christian, Kiao Inthavong, Wolfgang Sanz, and Jiyuan Tu. "Evaluation and improvements of RANS turbulence models for linear diffuser flows." *Computers & fluids* 71 (2013): 272-282.  
<https://doi.org/10.1016/j.compfluid.2012.10.015>.
- [12] Yang, Caiqing, Xudong Yang, and Bin Zhao. "The ventilation needed to control thermal plume and particle dispersion from manikins in a unidirectional ventilated protective isolation room." In *Building Simulation*, vol. 8, no. 5, pp. 551-565. Tsinghua University Press, 2015.  
<https://doi.org/10.1007/s12273-014-0227-6>.
- [13] Yakhot, V. S. A. S. T. B. C. G., S. A. Orszag, Siva Thangam, T. B. Gatski, and C. G. Speziale. "Development of turbulence models for shear flows by a double expansion technique." *Physics of Fluids A: Fluid Dynamics* 4, no. 7 (1992): 1510-1520.  
<https://doi.org/10.1063/1.858424>
- [14] Sadrizadeh, S., S. Holmberg, and A. Tammelin. "A comparison of vertical and horizontal laminar ventilation systems in an operating room: A numerical study." *Build. Environ* 82 (2014): 517-525.  
<https://doi.org/10.1016/j.buildenv.2014.09.013>
- [15] Nielsen, Peter Vilhelm. "Specification of a Two-Dimensional Test Case: (IEA)." Institut for Bygningsteknik, Aalborg Universitet, (1990).  
<https://www.forskningsdatabasen.dk/en/catalog/2389380067>
- [16] Nielsen, Peter V., Li Rong, and Inés Olmedo. "The iea annex 20 two-dimensional benchmark test for cfd predictions." In *Clima 2010*, pp. 165-166. Clima 2010: 10th Rehva World Congress, 2010.  
<https://vbn.aau.dk/en/publications/the-iea-annex-20-two-dimensional-benchmark-test-for-cfd-predictio-2>.
- [17] Cao, Zhixiang, Yi Wang, Chao Zhai, and Meng Wang. "Performance evaluation of different air distribution systems for removal of concentrated emission contaminants by using vortex flow ventilation system." *Building and Environment* 142 (2018): 211-220.  
<https://doi.org/10.1016/j.buildenv.2018.06.025>
- [18] Zhang, Zhao, Wei Zhang, Zhiqiang John Zhai, and Qingyan Yan Chen. "Evaluation of various turbulence models in predicting airflow and turbulence in enclosed environments by CFD: Part 2—Comparison with experimental data from literature." *Hvac&R Research* 13, no. 6 (2007): 871-886.  
<https://www.tandfonline.com/doi/citedby/10.1080/10789669.2007.10391460>